

A Time-domain Simulation Method for Hydroelastic Impact Problem

Katsuji Tanizawa

Ship Research Institute, Shinkawa, Mitaka, Tokyo, Japan

ABSTRACT: The aim of this study is development of a fully nonlinear time-domain simulation method for the analysis of transient hydroelastic problem with free-surface. As the first stage of this work, a nonlinear fluid and elastic body interaction problem is formulated in both the velocity and the acceleration field. In the formulation, the ideal fluid is assumed and the interaction between fluid and elastic vibration superposed on large amplitude solid mode body motions is taken into consideration. Based on this formulation, a two dimensional simulation program is developed. In the simulation program, BEM is used to solve the velocity and acceleration field and MEL is used to trace free-surface motion. Using this simulation program, two dimensional elastic beam impact on a wave crest is simulated as a test trial and effect of elasticity to the impact is confirmed.

1 INTRODUCTION

Ships and ocean structures have elastic body in the real world, but they are usually treated as solid in popular seakeeping theories for simplicity. When the scale of these structures are small, this simplification is considered to be valid. But, as the scale of the structure enlarged, relative rigidity of the body decrease and so elasticity becomes important. For wave radiation and diffraction problem of large scale floating structure, elastic response plays more important roll than solid mode body motions. Elastic response of floating airport is a good example. Even if the scale is small, elastic response can not be neglected when wave load is large. Water surface impact is the typical problem we should consider the elastic response.

Water surface impact causes the extreme hydrodynamic load and damages marine structures such as ships and oil platforms. For the safety design of the marine structures, the impact phenomena have been studied by many researchers theoretically, experimentally and numerically. In previous many studies, structures are assumed to be rigid and hydroelastic deformation and vibration are neglected for simplicity.

However, for the design of recent high speed vessels, hydroelastic analysis is required to estimate more accurate impact loads and elastic responses. Kvalsvold & Faltinsen (1995) and Faltinsen (1997) studied the effect of hydroelasticity on wetdeck slamming by a hydroelastic beam model. Khabakhpasheva & Korobkin (1997) studied wave impact on elastic plate by linear theory. Arai & Miyauchi (1997) simulated hydroelastic impact on cylindrical shell by finite difference method. Sumi et

al. (1997) experimentally studied water impact of elastic plate with small deadrise angles. Toyama (1998) extended Wagner's impact theory to hydroelastic impact problem and analyzed hydroelastic responses of cylindrical shell and cross deck panel to slamming.

Stimulated by these studies on hydroelastic impact problems, the author (1997b) formulated the nonlinear interaction between fluid and elastic body motions without free-surface and the confirmed the formulation by numerical simulation of Euler beam vibration in unbounded fluid up to 9th mode. This work was an extension of author's study (1997a) on nonlinear theory of wave-body interaction based on acceleration potential. Based on these studies, nonlinear fluid and elastic body interaction problem with free-surface is formulated in this paper. In the formulation, interaction between fluid and elastic vibration superposed on large amplitude solid mode body motions is considered. A two dimensional simulation program is developed to validate the formulation and a two dimensional elastic beam impact on a wave crest is simulated as a test trial. Simulated water surface impact is very transient. In the impact process, as wetted surface expands, added mass increases rapidly, the narrow peak impact pressure zone travels with very high speed and hydroelastic deformation takes place. Although the presented result in this paper is just a test trial of the simulation program and the resolution is not enough to catch the detail of the phenomenon, effect of elasticity to the impact is clearly observed and strong correlation between pressure and normal acceleration of vibration is confirmed.

2 GENERAL FORMULATION OF FLUID AND ELASTIC BODY INTERACTION PROBLEM

2.1 Velocity and acceleration of fluid on a elastic body surface

As illustrated in Fig.1, $O - XYZ$ is the space fixed reference frame and $o - xyz$ is the body fixed reference frame which origin o is fixed at the center of gravity. \mathbf{R} , \mathbf{R}_o and \mathbf{r} are positioning vectors. Motion of elastic body is assumed to be expressed by superposition of elastic vibration on the solid mode motions (simply written as vibration and motions in the following formulation). P is a point fixed to the fluid sliding on the body surface. Using the positioning vectors, the position, velocity and acceleration of point P can be written as

$$\mathbf{R} = \mathbf{R}_o + \mathbf{r} \quad (1)$$

$$\dot{\mathbf{R}} = \dot{\mathbf{R}}_o + \dot{\mathbf{r}} = \dot{\mathbf{R}}_o + \boldsymbol{\omega} \times \mathbf{r} + \langle \dot{\mathbf{r}} \rangle \quad (2)$$

$$\ddot{\mathbf{R}} = \ddot{\mathbf{R}}_o + \ddot{\mathbf{r}} = \ddot{\mathbf{R}}_o + \dot{\boldsymbol{\omega}} \times \mathbf{r} + \langle \ddot{\mathbf{r}} \rangle + \boldsymbol{\omega} \times (\boldsymbol{\omega} \times \mathbf{r}) + 2\boldsymbol{\omega} \times \langle \dot{\mathbf{r}} \rangle \quad (3)$$

where $\dot{\mathbf{R}}_o$ and $\boldsymbol{\omega}$ are translating and angular velocity of the body and $\langle \dot{\mathbf{r}} \rangle$ and $\langle \ddot{\mathbf{r}} \rangle$ are velocity and acceleration of point P observed from $o - xyz$ frame respectively.

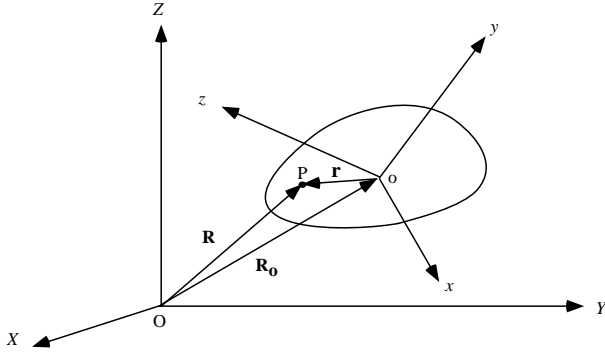


Fig. 1: Frame of reference

2.2 Boundary value problems of fluid domain

Ideal fluid is assumed and the velocity potential ϕ and the nonlinear acceleration potential

$$\Phi = \frac{\partial \phi}{\partial t} + \frac{1}{2}(\nabla \phi)^2 \quad (4)$$

are introduced to describe the fluid motion. This nonlinear acceleration potential is used by Tanizawa (1995) for nonlinear simulation of floating body motions. Similar to that $\nabla \phi$ gives fluid velocity, $\nabla \Phi$ gives fluid acceleration. Using these relations, the kinematic boundary

condition of the velocity potential and the acceleration potential can be written as

$$\phi_n = \mathbf{n} \cdot \dot{\mathbf{R}} \quad (5)$$

$$\Phi_n = \mathbf{n} \cdot \ddot{\mathbf{R}}, \quad (6)$$

where $\phi_n = \partial \phi / \partial n$, $\Phi_n = \partial \Phi / \partial n$ and \mathbf{n} is the normal vector of body surface.

Substituting (2) into (5) and (3) into (6), we have following boundary conditions.

$$\phi_n = v_n + \mathbf{n} \cdot \langle \dot{\mathbf{r}} \rangle \quad (7)$$

$$\Phi_n = a_n + \mathbf{n} \cdot \langle \ddot{\mathbf{r}} \rangle + \mathbf{n} \cdot \boldsymbol{\omega} \times (\boldsymbol{\omega} \times \mathbf{r}) + \mathbf{n} \cdot 2\boldsymbol{\omega} \times \langle \dot{\mathbf{r}} \rangle \quad (8)$$

where v_n and a_n are normal component of velocity and acceleration of body surface due to body motions respectively. v_n and a_n are given as

$$v_n = \mathbf{n} \cdot (\dot{\mathbf{R}}_o + \boldsymbol{\omega} \times \mathbf{r}) \quad (9)$$

$$a_n = \mathbf{n} \cdot (\ddot{\mathbf{R}}_o + \dot{\boldsymbol{\omega}} \times \mathbf{r}). \quad (10)$$

In case of solid body, the term $\mathbf{n} \cdot \langle \dot{\mathbf{r}} \rangle$ in (7) disappears because of orthogonality between \mathbf{n} and $\langle \dot{\mathbf{r}} \rangle$. But in case of elastic body, $\langle \dot{\mathbf{r}} \rangle$ has normal component caused by vibration. Here, the normal displacement of the body surface u is introduced. Using u , we have

$$\mathbf{n} \cdot \langle \dot{\mathbf{r}} \rangle = u_t \quad (11)$$

$$\mathbf{n} \cdot \langle \ddot{\mathbf{r}} \rangle = u_{tt} - k_n \langle \dot{\mathbf{r}} \rangle^2, \quad (12)$$

where $u_t = \partial u / \partial t$, $u_{tt} = \partial^2 u / \partial t^2$ and k_n is normal curvature of the body.

Taking these relations into account, the explicit kinematic boundary conditions on the elastic body surface

$$\{\phi_n\} = \{v_n\} + \{u_t\} \quad (13)$$

$$\{\Phi_n\} = \{a_n\} + \{u_{tt}\} + \{q\} \quad (14)$$

are derived, where

$$q = \mathbf{n} \cdot \boldsymbol{\omega} \times (\boldsymbol{\omega} \times \mathbf{r}) + \mathbf{n} \cdot 2\boldsymbol{\omega} \times \langle \dot{\mathbf{r}} \rangle - k_n \langle \dot{\mathbf{r}} \rangle^2 \quad (15)$$

is normal component of acceleration due to fluid flow and it can be evaluated from the solution of velocity field. In (13) and (14), variables are put into $\{array formula\}$ to explicitly show that these boundary conditions are applied every collocational points on wetted body surface.

2.3 Acceleration of body surface due to solid mode motions

The generalized equation of body motion is written as

$$\mathcal{M} \cdot \boldsymbol{\alpha} + \boldsymbol{\beta} = \mathbf{F}, \quad (16)$$

where \mathcal{M} , $\boldsymbol{\alpha}$ and \mathbf{F} are generalized inertia tensor, acceleration and external forces respectively and $\boldsymbol{\beta}$ is a

term so called Gyro-moment. In two dimensional case, $\beta = 0$. Introducing the generalized normal vector $\mathbf{N} = (\mathbf{n}, \mathbf{r} \times \mathbf{n})$, the generalized hydrodynamic force can be written as

$$\mathbf{F}_f = \int_s p \mathbf{N} ds = \int_s (-\Phi - Z) \mathbf{N} ds, \quad (17)$$

where integral is taken on the wet surface s . Denoting the other forces (thrust, gravity etc.) as \mathbf{F}_g , total force acts on the body is written as

$$\mathbf{F} = \mathbf{F}_f + \mathbf{F}_g = \int_s (-\Phi - Z) \mathbf{N} ds + \mathbf{F}_g. \quad (18)$$

Using these equations, the normal component of body surface acceleration due to body motions is obtained.

$$\begin{aligned} a_n &= \mathbf{N} \cdot \boldsymbol{\alpha} \\ &= \mathbf{N} \mathcal{M}^{-1} \left\{ \int_s (-\Phi - Z) \mathbf{N} ds + \mathbf{F}_g + \boldsymbol{\beta} \right\} \end{aligned} \quad (19)$$

Using boundary elements, (19) can be discretized and written in matrix form

$$\{a_n\} = [A]\{\Phi\} + \{B\}. \quad (20)$$

Detail of the above derivation is given by the author (1997a).

2.4 Acceleration of body surface due to vibration

It is not easy to formulate general equation of vibration for arbitrary elastic body. But, if we consider the discretized formula, the discretized equation of vibration can be generally written in following matrix form.

$$[\hat{\mathbf{M}}]\{\hat{u}_{tt}\} + [\hat{\mathbf{K}}]\{\hat{u}\} = [\hat{\mathbf{F}}]\{\hat{p}\} \quad (21)$$

In the equation, $\{\hat{u}\}$ is displacement of node points due to elastic vibration, $\{\hat{u}_{tt}\}$ is the second derivative of $\{\hat{u}\}$ with respect to time, $[\hat{\mathbf{M}}]$ is the mass matrix, $[\hat{\mathbf{K}}]$ is the rigidity matrix, $\{\hat{p}\}$ is pressure on the body surface and $[\hat{\mathbf{F}}]$ is transform matrix of pressure to equivalent lumped force on nodal points. In this paper, only pressure is considered as external force for simplicity. Hat mark ' $\hat{}$ ' above the variable means the values are given with respect to the node points of elastic body discretization. If necessary, damping term can be added to the equation. Generally, this discretized equation can be derived from the principle of virtual work and popularly used in dynamic structure analysis by FEM. Solving the acceleration of vibration, we have

$$\{\hat{u}_{tt}\} = -[\hat{\mathbf{K}}_M]\{\hat{u}\} + [\hat{\mathbf{F}}_M]\{\hat{p}\}, \quad (22)$$

where $[\hat{\mathbf{K}}_M] = [\hat{\mathbf{M}}]^{-1}[\hat{\mathbf{K}}]$ and $[\hat{\mathbf{F}}_M] = [\hat{\mathbf{M}}]^{-1}[\hat{\mathbf{F}}]$.

The above formulations are general and valid not only for two dimensional problems but also for three dimensional problems. However, for more concrete discussion, the author restricts the problem to two dimension in the following part.

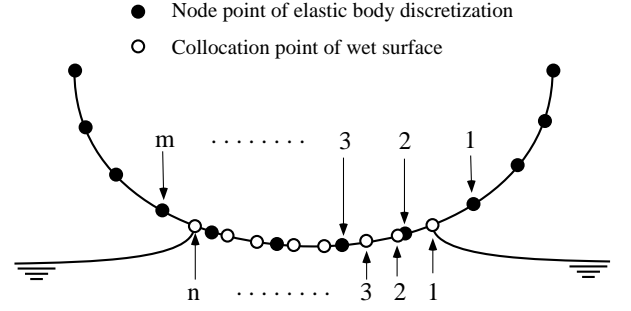


Fig. 2: Explanatory drawing of node points of elastic body discretization and collocation points on wet surface for fluid motion computation

Fig.2 is explanatory drawing of two dimensional hydroelastic problem. In the figure, white circles \circ are collocation points on the fluid boundary. These collocation points move as wet surface moves. On the other hand, black circles \bullet are node points of body surface discretization fixed to the body surface. Eq.(14) is composed with respect to the collocation points \circ , and eq.(22) is composed with respect to the node points \bullet . To combine these two equations, we need to derive the equation which gives the normal acceleration of the elastic body at \circ . From eq.(22), the subset of the equation related to the normal component of body surface at \bullet can be derived.

$$\{\hat{u}_{tt}\} = -[\hat{\mathbf{K}}_M]\{\hat{u}\} + [\hat{\mathbf{F}}_M]\{\hat{p}\} \quad (23)$$

where $\{\hat{u}\}$ and $\{\hat{u}_{tt}\}$ are normal component to body surface extracted from $\{\mathbf{u}\}$ and $\{\mathbf{u}_{tt}\}$, respectively. $[\hat{\mathbf{K}}_M]$ and $[\hat{\mathbf{F}}_M]$ are subset of $[\hat{\mathbf{K}}_M]$ and $[\hat{\mathbf{F}}_M]$ related to the normal component. In general, rotational transform is required to obtain eq.(23) from eq.(22).

Next, we need to obtain the value of $\{u_{tt}\}$ at \circ by interpolating the values of $\{\hat{u}_{tt}\}$ at \bullet . For this interpolation, the minimum set of node points numbered from 1 to m in Fig.2 are selected and interpolation matrix $[IP]$ of n row m column is introduced, where n is the number of collocation points on the wet surface. Calculation of $[IP]$ matrix and its regularity are discussed in the appendix. Again, the subset of equation only related to $\hat{u}_i, i = 1 \sim m$ is extracted from eq.(23) for the interpolation.

$$\{\hat{u}'_{tt}\} = -[\hat{\mathbf{K}}'_M]\{\hat{u}'\} + [\hat{\mathbf{F}}'_M]\{\hat{p}'\}, \quad (24)$$

where dash ' ' denotes the subset corresponds to the minimum set of node points for the interpolation. Using $[IP]$, $\{u_{tt}\}$ can be written as

$$\{u_{tt}\} = [IP]\{\hat{u}'_{tt}\}. \quad (25)$$

Next, inverse operation of the interpolation is required. Since $[IP]$ is not a square matrix, we have to

consider general inverse matrix. When matrix $[IP]^{-1}$ satisfies

$$\left. \begin{array}{l} (a) [IP][IP]^{-1}[IP] = [IP] \\ (b) [IP]^{-1}[IP][IP]^{-1} = [IP]^{-1} \\ (c) ([IP]^{-1}[IP])^T = [IP]^{-1}[IP] \\ (d) ([IP][IP]^{-1})^T = [IP][IP]^{-1} \end{array} \right\} \quad (26)$$

$[IP]^{-1}$ is called Moore-Penrose general inverse matrix and conventionally written as $[IP]^+$. $[IP]^+$ is the unique inverse matrix of m row n column. If Moore-Penrose general inverse matrix $[IP]^+$ exists, the inverse operation of interpolation is very accurate. Fortunately, we can apply next theorem to obtain $[IP]^+$.

$$[IP]^+ = ([IP]^T[IP])^{-1}[IP]^T, \quad \text{when Rank}([IP]) = m \quad (27)$$

$$[IP]^+ = [IP]^T([IP]^T[IP])^{-1}, \quad \text{when Rank}([IP]) = n. \quad (28)$$

Detail of Moore-Penrose general inverse matrix is explained by Okamoto, (1992).

Using $[IP]^+$, $\{\hat{p}'\}$ is written as

$$\{\hat{p}'\} = [IP]^+ \{p\}. \quad (29)$$

Then, multiplying eq.(24) by $[IP]$ and using eq.(25) and eq.(29), the values of u_{tt} at \circ is obtained as follows,

$$\{u_{tt}\} = -[IP][\hat{K}'_M]\{\hat{u}'\} + [IP][\hat{F}'_M][IP]^+ \{p\}. \quad (30)$$

Substituting $p = -\Phi - Z$ into (30), finally we have the linear relational expression between acceleration of vibration and the acceleration potential

$$\{u_{tt}\} = [C]\{\Phi\} + \{D\} \quad (31)$$

$$[C] = -[IP][\hat{F}'_M][IP]^+ \quad (32)$$

$$\{D\} = -[IP][\hat{K}'_M]\{\hat{u}'\} + [C]\{Z\}. \quad (33)$$

2.5 Implicit body surface boundary condition of Φ

Normal acceleration a_n and u_{tt} in the boundary condition (14) are unknown, but these values can be determined by solving the simultaneous equation of fluid and elastic body motions using the implicit boundary condition. Substituting (20) and (31) into (14), we can eliminate unknown a_n and u_{tt} and obtain the implicit boundary condition.

$$\{\Phi_n\} = [A + C]\{\Phi\} + \{B + D + q\} \quad (34)$$

This implicit condition prescribes the relation between the acceleration potential Φ and its flux Φ_n . Since this condition is derived from both kinematic boundary condition of Φ and equations of body motions and elastic vibration, this is kinematic and at the same time dynamic boundary condition which connects the fluid and elastic body motions. Using this implicit boundary condition, we can solve fluid and elastic body interaction problem without modal decomposition.

2.6 Numerical procedures to simulate hydroelastic problem

To solve the boundary value problem (BVP) with boundary element method (BEM), the acceleration potential Φ is not adequate because Φ dose not satisfy Laplace equation. However, BVP of Φ can be easily converted to BVP of $\phi_t (\equiv \partial\phi/\partial t)$, which satisfy Laplace equation. Therefore BVP of ϕ and ϕ_t are solved for numerical simulation in this paper.

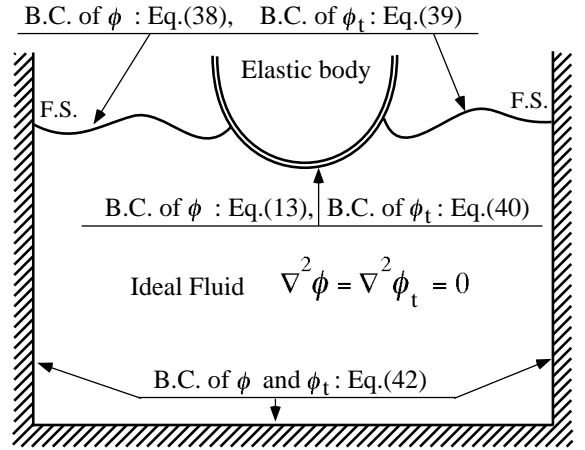


Fig. 3: Boundary value problem

Fig.3 is an illustration of BVP. From Green's second identity, we have

$$c(\mathcal{Q}) \begin{Bmatrix} \phi(\mathcal{Q}) \\ \phi_t(\mathcal{Q}) \end{Bmatrix} = \int_S \begin{Bmatrix} \phi(\mathcal{P}) \\ \phi_t(\mathcal{P}) \end{Bmatrix} \frac{\partial}{\partial n} \ln R(\mathcal{P}, \mathcal{Q}) - \ln R(\mathcal{P}, \mathcal{Q}) \begin{Bmatrix} \frac{\partial \phi(\mathcal{P})}{\partial n} \\ \frac{\partial \phi_t(\mathcal{P})}{\partial n} \end{Bmatrix} dS \quad (35)$$

where \mathcal{P}, \mathcal{Q} are points on the boundary and c is the external angle of the boundary at the point \mathcal{Q} .

Using BEM, discretized matrix form of eq.(35)

$$[H] \{\phi\} = [G] \{\phi_n\} \quad (36)$$

$$[H] \{\phi_t\} = [G] \{\phi_{tn}\} \quad (37)$$

are obtained and BVP can be solved with following boundary conditions.

The free-surface boundary condition of ϕ and ϕ_t are

$$\phi = \int_0^t \frac{1}{2} (\nabla \phi)^2 - gZ dt \quad (38)$$

$$\phi_t = -\frac{1}{2} (\nabla \phi)^2 - gZ, \quad (39)$$

where the time integral is performed tracing the material fluid particle. Kinematic condition is also satisfied by tracing the particle motion on the free-surface. Namely, Mixed Eulerian-Lagrangian method (MEL) is

used. For hydroelastic wave radiation and diffraction problem, radiation condition is necessary. The radiation condition can be satisfied by introducing the artificial damping term in the free-surface boundary condition (Tanizawa 1997a).

The elastic body surface boundary condition of ϕ is given by eq.(13) and the implicit body surface boundary condition of ϕ_t is given by substituting eq.(4) into eq.(34).

$$\{\phi_{tn}\} = [A + C]\{\phi_t\} + \{B + D + q'\} \quad (40)$$

$$q' = q + [A + C]\left\{\frac{1}{2}(\nabla\phi)^2\right\} - \frac{\partial}{\partial n} \left\{\frac{1}{2}(\nabla\phi)^2\right\} \quad (41)$$

The term q' can be explicitly evaluated from the solution of BVP of ϕ .

On the straight bottom and the straight vertical walls, simple kinematic boundary condition

$$\phi_n = \phi_{tn} = 0 \quad (42)$$

can be applied.

Fig.4 shows the flow chart of the simulation method. First, started from given initial boundary shape and initial conditions, the discretized equations, eq.(36),(37), (23) are composed.

Next, interpolation matrix and its Moore-Penrose general inverse matrix is composed, boundary conditions of ϕ are determined and BVP of ϕ is solved.

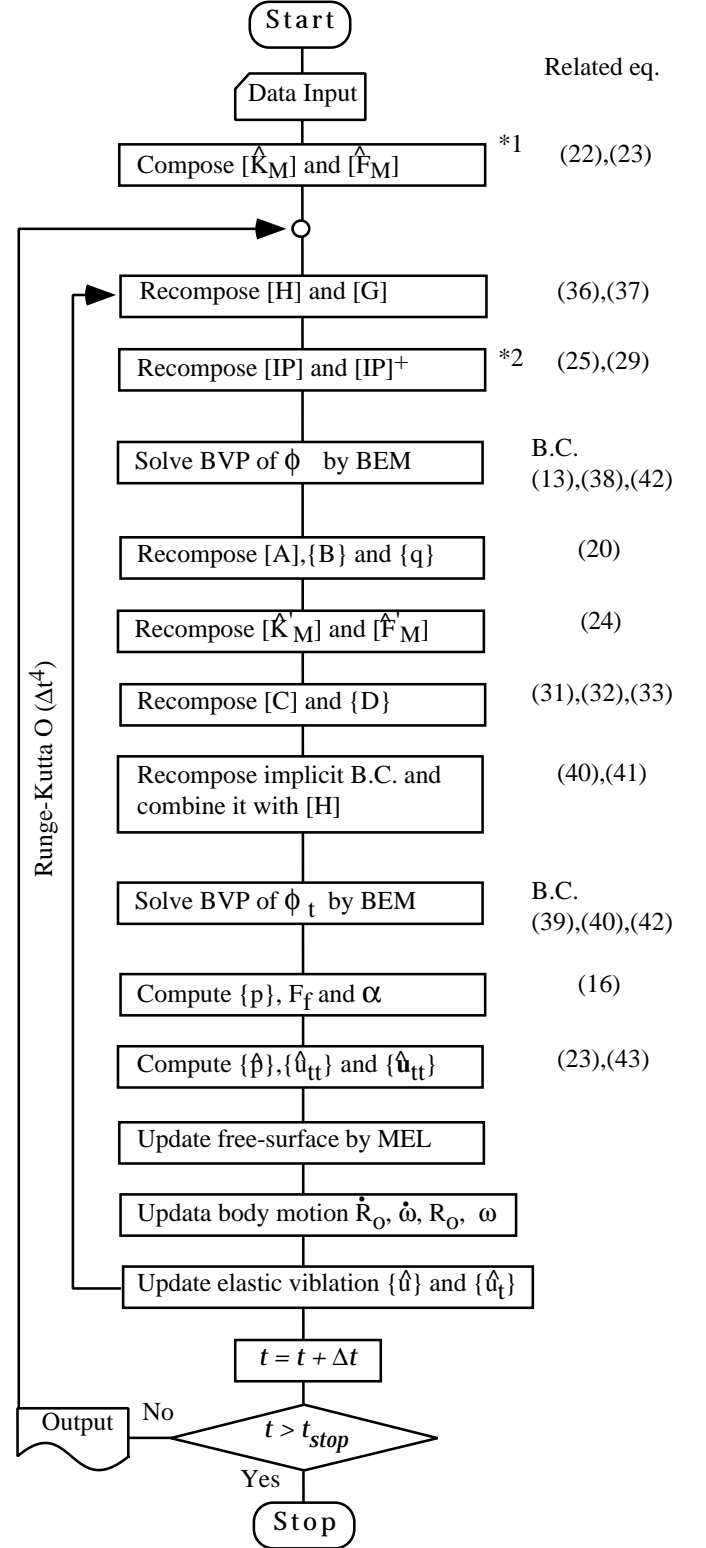
Using the solution of ϕ , the boundary conditions of ϕ_t are calculated from eq.(39),(40) and (42). BVP of ϕ_t is solved, next.

From the solution of ϕ_t , pressure distribution of the elastic body surface $\{p\}$ and hydrodynamic forces \mathbf{F}_f are obtained. The acceleration of solid mode body motion α is calculated from eq.(16). The acceleration of vibration $\{\hat{u}_{tt}\}$ is calculated from eq.(22) and eq.(29).

Using MEL, position and value of ϕ of the free-surface are updated. And time integral of body acceleration gives the velocity of the body and displacement of body for next time step. 4th order Runge-Kutta method is used for numerical time integral.

3 SIMULATION OF WATER SURFACE IMPACT

As a test trial of this simulation method, two dimensional water surface impact of a Euler beam is simulated. Fig.5 shows the instance of the contact. The beam falls with constant velocity $V = 1$ and contacts with the free-surface at its center. The both ends of the beam are fixed with rigid body. To simplify the problem, span of the beam L , rigidity of the beam EI , linear density of the beam (mass of the beam per unit length) $\rho_b h$, density of fluid ρ_f , gravitational acceleration g are all set to 1. All values in this paper are nondimensionalized using ρ_f , g and L as units.



*1 If elastic deformation is large, $[\hat{K}_M]$ and $[\hat{F}_M]$ should be recomposed every time steps

*2 See appendix

Fig. 4: Flow of the simulation

For the numerical simulation, the beam is evenly segmented to 10 elements. Number of collocation points for fluid simulation are 40 on free-surface, 20 on wetted beam surface and 30 on the other boundaries.

The free-surface motion before the contact is plotted in Fig.6. This motion is obtained by the nonlinear simulation of fluid from calm condition with given initial free-surface elevation $\eta(x)_{t=0} = 0.1 \cos(2\pi x)$. The average depth of water is also set to 1. At the instance of contact, nondimensional time $t = 0.7$, the rising velocity of the center of free-surface is 0.3367. Therefore impact velocity between free-surface and the beam is 1.3367.

Fig.7 shows the simulated free-surface after the contact. At the instance of contact, the span of wetted part should be zero. However, this condition is hard to impose on the numerical simulation. Therefore a small part of wave crest is cut to have finite wetted span, $\Delta x \approx 0.03$. For the simulation of impact phase, very thin spray is also an obstacle. Thin spray layer on the beam surface is also cut during the simulation. The impact phase simulation is roughly achieved in such a way.

Fig.8 shows the impact pressure distributions on the elastic beam (solid line) and rigid beam (broken line). To observe the elastic effect, a rigid beam impact $EI = \infty$ is also simulated using the same code. Fluctuation of the solid line around the broken line is observed from $t = 0.712$ to $t = 0.720$. This fluctuation is caused by hydroelastic effect.

Next, the elastic beam deformation is plotted in Fig.9. At $t = 0.732$ two peaks are observed. This peaks are considered to due to third mode of vibration and not due to static response to the pressure distribution shown in Fig.8.

The time histories of u and u_{tt} at $x = 0.1 \sim 0.5$ are plotted in Fig.10 and Fig.11, and the pressure time history on the elastic beam and rigid beam at $x = 0.4 \sim 0.5$ are plotted in Fig.13 and Fig.12, respectively. At the initial stage of the impact, very high impact pressure appears. This high pressure is caused by singular initial condition of the impact simulation, i.e. due to the cut of the small part of wave crest at the beginning. Consequently, the maximum value of the impact pressure is not reliable. For more accurate simulation, the analytical solution should be applied to the initial condition (Zhang, 1996). However, except the initial stage of the impact, impact pressures on both elastic beam and rigid beam are reasonable. In Fig.12, the effect of beam vibration on impact pressure can be observed. Comparing the impact pressure and the acceleration of beam vibration in Fig.11 at $x = 0.5$, we can recognize the strong correlation between them.

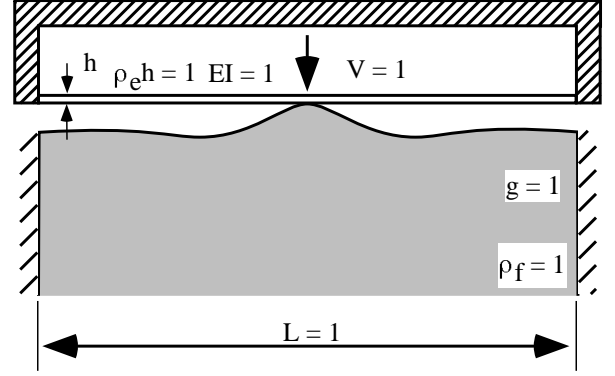


Fig. 5: Simulation of Euler beam impact on a wave crest

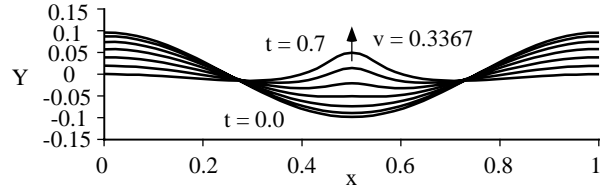


Fig. 6: Free-surface motion before the contact

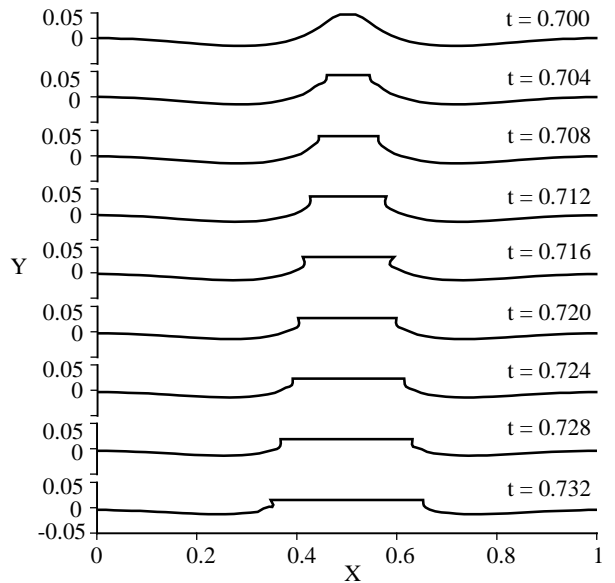


Fig. 7: Free-surface motion after the contact

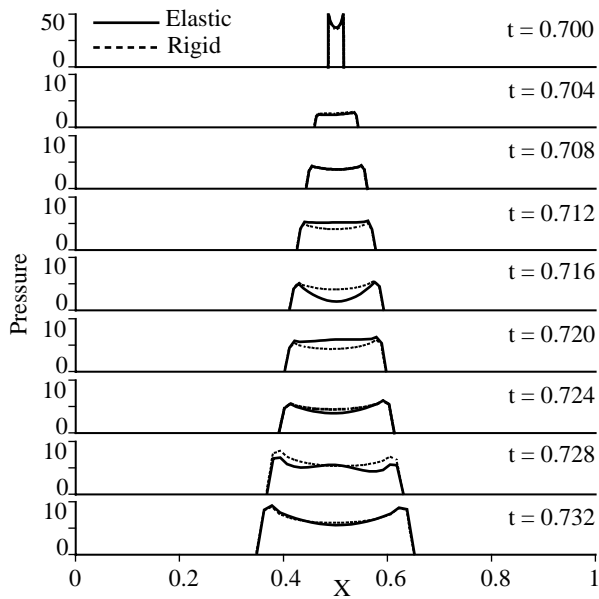


Fig. 8: Impact pressure distribution

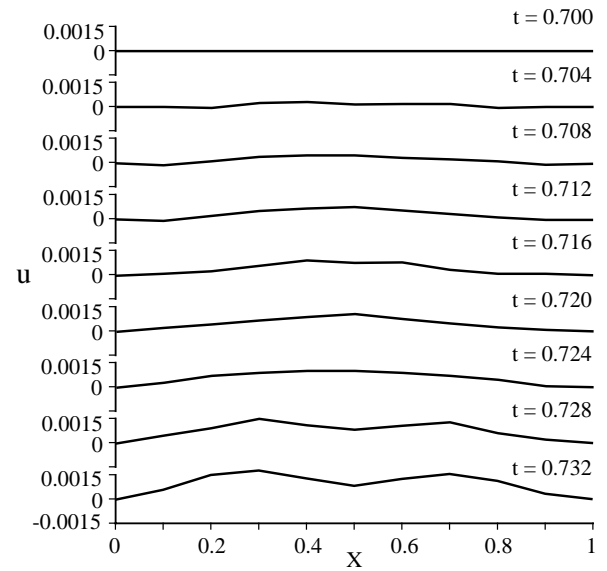


Fig. 9: Beam distortion during the impact

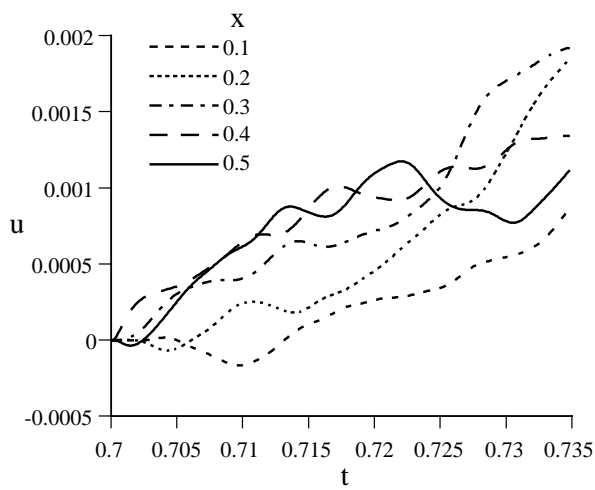


Fig. 10: Time history of beam vibration : u

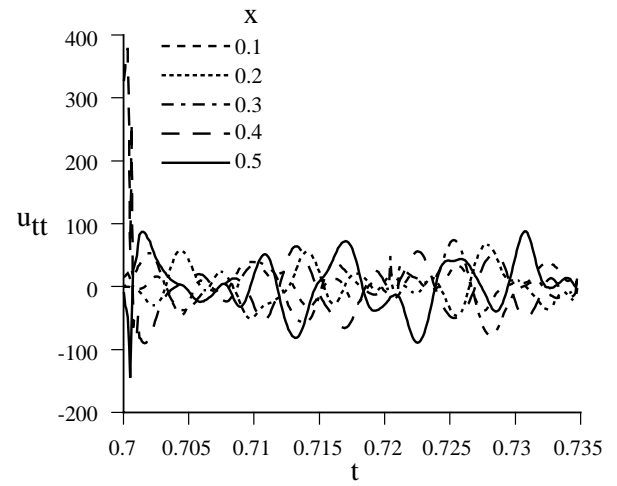


Fig. 11: Time history of beam vibration acceleration u_{tt}

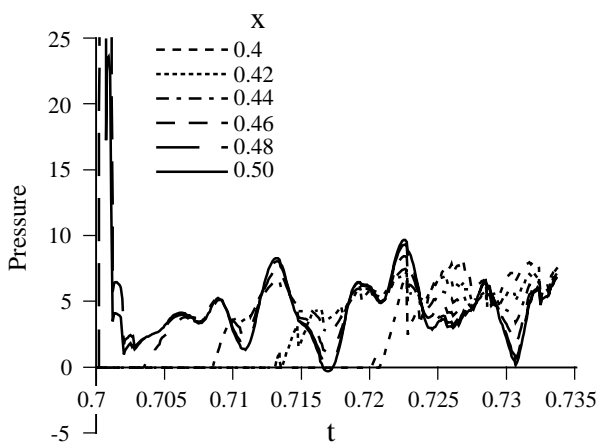


Fig. 12: Time history of hydroelastic impact pressure

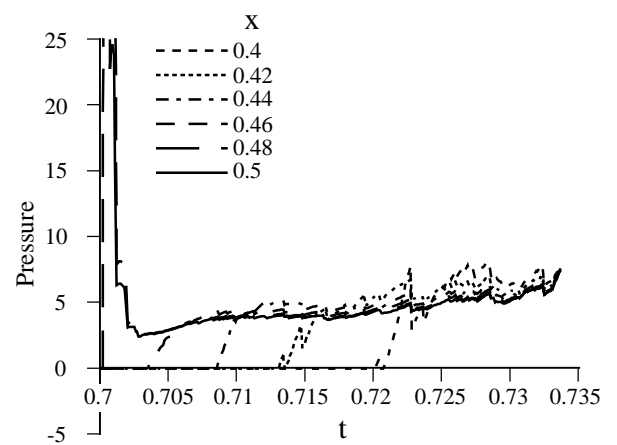


Fig. 13: Time history of rigid body impact pressure

4 CONCLUSION

In this study, a nonlinear fluid and elastic body interaction problem with free-surface is formulated, a numerical simulation program for hydroelastic impact problem is developed and a two dimensional free-surface impact problem of Euler beam is simulated. Following items are main results of this study.

1. The exact kinematic boundary conditions on elastic body surface are derived for the velocity potential ϕ and the acceleration potential Φ .
2. Relational expression between Φ and body surface normal acceleration due to elastic vibration u_{tt} are derived.
3. For numerical simulation, interpolation and its inverse operation techniques are developed using the cubic spline interpolation matrix and Moore-Penrose general inverse matrix.
4. The implicit boundary condition of Φ on elastic body surface is derived.
5. A nonlinear simulation program based on this formulation is developed.
6. As a test trial of the simulation method, a hydroelastic impact of Euler beam is simulated and the interaction between elastic vibration and the impact pressure is confirmed.

This study is a part of my plan to develop fully nonlinear numerical wave tank for ship seakeeping problem. This nonlinear simulation method can be applied not only to impact problem but also to various hydroelastic problems.

REFERENCES

- Kawai,T. and Muraki,T., 1969, "Matrix method of Analysis of ship structure (IV)", *J. Soc. Nav. Arch. Japan*, vol.126, pp245-252
- Kawai,T., 1970, "Matrix method for vibration and elastic response (in Japanese)", *Baifu-kan*, pp1-235
- Kito,F., 1970, "Principles of hydro-elasticity", *Yokendo*, pp1-129
- Okamoto,Y., 1992, "How to solve inverse problem (in Japanese)", *Ohmu-sha*,pp1-238
- Tanizawa,K., 1995, "A Nonlinear Simulation Method of 3-D body Motions in Waves", *J. Soc. Nav. Arch. Japan*, vol.178, pp179-191
- Kvalsvold,J. and Faltinsen,O., 1995 "Hydroelastic modeling of wetdeck slamming on multihull vessels" *J Ship Res.*, vol.39, pp225-229
- Zhang,S., Yue,D.K.P. and Tanizawa,K., 1996 "Simulation of plunging wave impact on a vertical wall" *J Fluid Mech.*, vol.327, pp221-254
- Khabakhpasheva,T.I. and Korobkin,A.A., 1997 "Wave impact on elastic plates ", *Proc. 12th Int. Workshop on Water Waves and Floating Bodies*,pp135-138

Tanizawa,K., 1997a, "Nonlinear theory of wave-body interaction based on acceleration potential and its application to numerical simulation (in Japanese)", *Ph.D thesis, Osaka Univ.*, pp1-127

Tanizawa,K., 1997b, "A nonlinear simulation method of hydro-elastic problem", *Proc. Simp.on Non-linear and Free-Surface Flow*, Hiroshima, Japan

Faltinsen,O.M., 1997, "The effect of hydroelasticity of ship slamming", *Phil. Trans. R. Soc. Lond. A*, vol.355, pp575-591

Sumi,Y.,Okada,S.,Mukai,H. and Inoue,K. 1997, "Study on water impact of elastic plate with small deadrise angles (in Japanese)", *J. Soc. Nav. Arch. Japan*, vol.182, pp639-646

Arai,M. and Miyauchi,T., 1997, "Numerical simulation of the water impact on cylindrical shells considering fluid-structure interaction", *J. Soc. Nav. Arch. Japan*, vol.182, pp827-835

Toyama,Y., 1998, "Hydroelastic response of cross deck panel to slamming", *J. Soc. Nav. Arch. Japan*, vol.183, pp417-423

APPENDIX : Interpolation matrix based on cubic-B spline

Interpolation of a single value function $f(x)$ with given sample points $\{\hat{f}\} = \{f(\hat{x}_1), f(\hat{x}_2), \dots, f(\hat{x}_m)\}^T$ is considered, where ' ^ ' denotes the original sample points, see Fig.A-1. In the appendix, $f(\hat{x}_i)$ is simply written as \hat{f}_i . Basic idea of cubic-B spline interpolation is obtaining the approximation function as the summation of piecewise cubic tent functions

$$f(x) \approx \sum_{i=1}^m w_i B_i(x), \quad (\text{A-1})$$

where w_i is weight and $B_i(x)$ is the piecewise cubic tent function

$$B_i(x) = \begin{cases} 0 & x < x_{i-2} \\ b_{1i}(x) & x_{i-2} \leq x < x_{i-1} \\ b_{2i}(x) & x_{i-1} \leq x < x_i \\ b_{3i}(x) & x_i \leq x < x_{i+1} \\ b_{4i}(x) & x_{i+1} \leq x < x_{i+2} \\ 0 & x_{i+2} \leq x \end{cases} \quad (\text{A-2})$$

$$b_{1i}(x) = \frac{(x - x_{i-2})^3}{(x_{i+1} - x_{i-2})(x_i - x_{i-2})(x_{i-1} - x_{i-2})} \quad (\text{A-3})$$

$$b_{2i}(x) = \frac{(x - x_{i-2})}{(x_{i+1} - x_{i-2})} \left\{ \frac{(x - x_{i-2})(x_i - x)}{(x_i - x_{i-2})(x_i - x_{i-1})} + \frac{(x_{i+1} - x)(x - x_{i-1})}{(x_{i+1} - x_{i-1})(x_i - x_{i-1})} \right\}$$

$$+ \frac{(x_{i+2} - x)(x - x_{i-1})^2}{(x_{i+2} - x_{i-1})(x_{i+1} - x_{i-1})(x_i - x_{i-1})} \quad (\text{A-4})$$

$$b_{3i}(x) = \frac{(x_{i+2} - x)}{(x_{i+2} - x_{i-1})} \left\{ \frac{(x - x_{i-1})(x_{i+1} - x)}{(x_{i+1} - x_{i-1})(x_{i+1} - x_i)} \right\}$$

$$+ \left. \frac{(x_{i+2} - x)(x - x_i)}{(x_{i+2} - x_i)(x_{i+1} - x_i)} \right\}$$

$$+ \frac{(x - x_{i-2})(x_{i+1} - x)^2}{(x_{i+1} - x_{i-2})(x_{i+1} - x_{i-1})(x_{i+1} - x_i)} \quad (\text{A-5})$$

$$b_{4i}(x) = \frac{(x_{i+2} - x)^3}{(x_{i+2} - x_{i-1})(x_{i+2} - x_i)(x_{i+2} - x_{i+1})} \quad (\text{A-6})$$

Substituting the sampling points \hat{x}_i , $i = 1 \sim m$ into eq.(A-1), a set of linear equation

$$\{\hat{f}\} = [\hat{S}]\{\hat{w}\} \quad (\text{A-7})$$

is obtained, where $\{\hat{w}\} = \{\hat{w}_1, \hat{w}_2, \dots, \hat{w}_m\}^T$ is an array of the weight and $[\hat{S}]$ is the cubic B-spline matrix which elements are calculated from the sampling points \hat{x}_i , $i = 1 \sim m$ and tent function $B_i(x)$. Solving eq.(A-7), weight is obtained as

$$\{\hat{w}\} = [\hat{S}]^{-1}\{\hat{f}\}. \quad (\text{A-8})$$

Now, we know $\{\hat{w}\}$. Using $\{\hat{w}\}$, interpolated value of function $f(x)$ at x_j can be given by eq.(A-1). Fig.A-3 shows the original sampling points \hat{x}_i , $i = 1 \sim m$ and the interpolated points x_j , $j = 1 \sim n$. Eq.(A-1) can be applied to all interpolated points and interpolated values $\{f\} = \{f_1, f_2, \dots, f_n\}^T$ also can be written in matrix form as

$$\{f\} = [S]\{\hat{w}\}, \quad (\text{A-9})$$

where spline matrix $[S]$ is n row m column and its elements are calculated from the both sampling points $\{\hat{x}_i\}$ and interpolated points $\{x_j\}$. Finally, combining eq.(A-8) and eq.(A-9), the linear relation between $\{f\}$ and $\{\hat{f}\}$ is obtained.

$$\{f\} = [S][\hat{S}]^{-1}\{\hat{f}\} = [IP]\{\hat{f}\} \quad (\text{A-10})$$

where $[IP] = [S][\hat{S}]^{-1}$ is the interpolation matrix.

$[IP]$ is n row and m column matrix and its Moore-Penrose general inverse matrix $[IP]^+$ is given by eq.(27) or eq.(28) unless $[IP]$ is singular. Fig.A-4 shows one bad choice of $\{\hat{x}\}$. In this case, $[IP]$ is singular and $[IP]^+$ dose not exist. The reason is very simple. As Fig.A-4 shows, the tent function $B_1(x)$ dose not cover any point of $\{x\}$. This means the point \hat{x}_1 is totally redundant for the interpolation, therefore value of \hat{f}_1 never affects to the interpolated values. As the consequence, $[IP]$ becomes singular and no unique inverse matrix exists. This is a typical bad example. In order to have $[IP]^+$, $\{\hat{x}\}$ should be selected carefully, so that no redundant points are included.

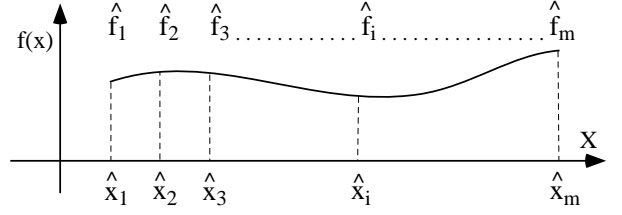


Fig. A-1: Sampling points of function $f(x)$

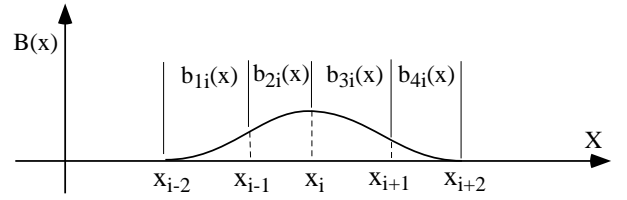


Fig. A-2: Cubic-B spline tent function

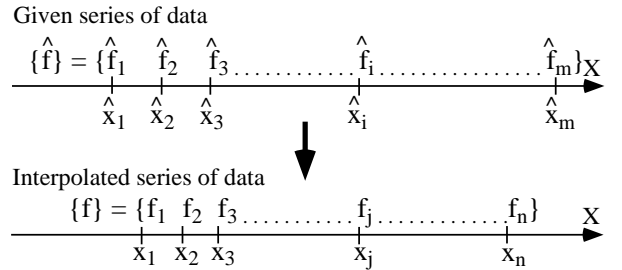


Fig. A-3: Sampling points and interpolated points

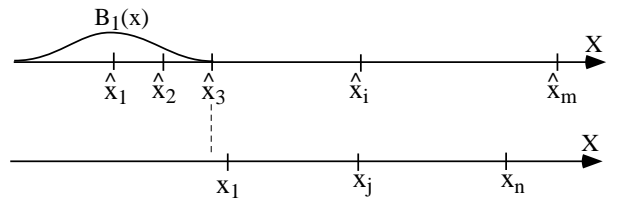


Fig. A-4: An example of bad choice of sampling points